Journal of Statistical Physics, Vol. 52, Nos. 5/6, 1988

Computer Simulations of the Growth of Breath Figures

Daniela Fritter,[1] Charles M. Knobler,[1] Didier Roux,[2] and Daniel Beysens[3]

Received April 26, 1988

We describe computer simulations of the growth of breath figures, the patterns formed when droplets condense on a cold surface. The focus is on the coalescence of droplets, which is an important growth mechanism, and the conditions for self-similar patterns, which are experimentally observed. It is assumed that individual droplets grow according to a power law; droplets that touch coalesce instantly and are replaced by a new droplet at the center of gravity of the coalescing pair. The average droplet radius, distribution of droplet sizes, surface coverage, and radial distribution function are determined as a function of the time for a variety of initial coverages and polydispersities. These quantities are compared to those determined by experiment, and our simple model is found to be in good accord with the observed behavior. It is observed that the process of coalescence induces spatial correlation between droplets.

KEY WORDS: Droplet growth; coalescence; simulation; surfaces; patterns.

1. INTRODUCTION

Breath figures are the patterns formed when droplets condense onto surfaces, usually glass. Early investigators[1] of the phenomenon observed that the haze formed when water vapor condensed onto glass surfaces was not uniform and it was determined that the patterns formed were controlled by the manner in which the surface was prepared. Later studies by Merigoux and co-workers[2-4] demonstrated that the formation of breath figures

This paper is dedicated to Howard Reiss on his 66th birthday.

[1] Department of Chemistry and Biochemistry, University of California, Los Angeles, California 90024.

[2] Centre P. Pascal, CNRS, Domaine Universitaire, 33404 Talence, France.

[3] Service de Physique du Solide et de Résonance Magnétique, CEN Saclay, 91191 Gif-sur-Yvette, France.

0022-4715/88/0900-1447$06.00/0

depends very sensitively on surface cleanliness. Water condenses as a film onto a clean glass surface but as droplets onto a glass surface that is coated by even a monolayer of a fatty acid.

More recent investigations of breath figures have focused on the kinetics of droplet growth. Using simultaneous microscopic and light-scattering measurements, Beysens and Knobler[5] studied the condensation of water droplets onto glass surfaces that had been silanized so that the contact angle was close to 90°. The experiments were carried out by allowing gas saturated with water vapor at room temperature to flow across the glass, which was cooled below room temperature. The supersaturation and flow rate remained constant throughout the experiment. With the microscopic observations they were able to resolve individual droplets with diameters as small as 2 μm and to follow their growth to sizes up to 300 μm. The light scattering studies provided complementary information about the growth of the ensemble of droplets.

In a typical experiment, after an initial brief period during which individual droplets cannot be seen and there is little light scattering, there follows a regime during which the growth behavior remains remarkably uniform. In this regime, called the intermediate regime by Beysens and Knobler, there are two distinct growth modes, which can easily be seen by following individual droplets. The radius of an isolated droplet follows a power law, $R \propto t^a$, with $a = 0.23$. When the droplet touches one or more other droplets, there is a rapid coalescence and the resulting larger droplet continues to grow with the same power law. The effects of these coalescences are seen in the more rapid growth of the average droplet radius $\langle R \rangle$, which also follows a power law but with an exponent $a' = 0.75$. The power-law exponents were found to be independent of the flux and the supersaturation.

Throughout the intermediate regime the fraction of the surface covered by droplets and the polydispersity remain constant at 0.55 and 0.20, respectively. The light scattering has the form of an annular ring with a maximum at a wave number k_m that decreases with time. Plots of the reduced intensity $I(k)/I(k_m)$ against the reduced wave number k/k_m are superimposable, demonstrating that the droplet pattern is self-similar.

The observed single-drop exponent a can be compared with values predicted by models of droplet growth. If a droplet grows by direct condensation of vapor onto its surface, then the change in volume with time must be proportional to R^2, hence $a = 1$. If the droplet is sufficiently large, a temperature gradient will exist in the droplet perpendicular to the substrate surface. The accommodation constant will then vary inversely with some characteristic length,[6] which may be taken as R, leading to $a = 1/2$. A growth mechanism in which critical nuclei condense on the substrate and

then diffuse to the periphery of droplets and coalesce[5] gives $a = 1/3$. Viovy *et al.*[7] considered the requirements for self-similar behavior in systems that grow by condensation and coalescence. They found that a necessary condition for self-similarity is $a = 1/3$ and they demonstrated that for self-similar growth, $a' = 3a$.

It remains unclear why the observed rate of growth is so slow, i.e., why the experimental value of a is so small. Further study of the growth of individual droplets needs to be undertaken. If one accepts, however, that droplets grow with a power law, one can ask how the properties of an ensemble of such droplets evolve when coalescences between growing droplets can take place. This is a formidable theoretical problem but one that is very easy to study by simulation. Such simulations are the subject of this paper.

2. THE MODEL

The basic procedure is to establish an initial configuration of disks on a planar surface. The time is then incremented and the radii of the disks increase according to a power law. When two disks touch, they coalesce and are replaced by a new disk whose radius is computed on the assumption that the disks represent sections of hemispheres. In the experiments, the new droplet is found to be centered at the center of mass of the coalescing pair. This is the location chosen in most of our simulations, but studies have also been carried out with a computationally simpler procedure in which the new droplet is centered on the site of the larger coalescing droplet. After the coalescence takes place a check is made for contacts with other droplets that occur as the result of the coalescence. When these have been dealt with, the time is again incremented and single-droplet growth continues until the next contact and coalescence. Periodic boundary conditions are utilized to eliminate edge effects.

Similar computations are described in the engineering literature.[6,8–10] The process of dropwise condensation is of engineering interest because the heat transfer coefficients when fluids condense as droplets are much higher than when they condense as films. In general, engineers have studied steady-state condensation, where droplets that reach a specified size (the "departure size") fall from the substrate (are removed from the simulation) and expose a clean surface on which small droplets can nucleate.

Gose *et al.*,[6] for example, considered a model in which there were 200 randomly positioned nucleation sites upon which droplets grew with a $t^{1/2}$ power law. They varied the droplet density by the choice of the departure size. Later, Tanasawa and Tachibana[8] used the same model but increased the number of sites to 3200. Both of these simulations led to heat transfer

coefficients more than an order of magnitude smaller than those observed experimentally.

An essential difficulty in the simulation of the steady state is the enormous range of sizes that must be accounted for; the ratio between the smallest and largest droplets is over three orders of magnitude. The overall condensation rate is strongly dependent on the evolution of the smallest droplets, yet the area to be analyzed must be large enough to yield a statistically valid sampling of the largest droplets.

Glicksman and Hunt[9] overcame this difficulty by simulating the condensation and coalescence process in a series of time and size stages, ranging from nucleation of equally sized, randomly located droplets to the formation of a droplet of the departure size. The growth of the large drops from an earlier stage is carried over into the next stage, which has an area ten times larger. The behavior of smaller droplets is accounted for by the average properties of the earlier stage. Thus only the growth and coalescence of the larger drops in any stage are treated in detail. With this procedure they were able to simulate site densities as large as $10^8\ \mathrm{cm}^{-2}$ while working with only 1000 sites.

Since the goal of the engineering simulations was to understand the heat transfer process, little if any attention was paid to the approach to the steady state. The steady-state process is not self-similar because of the nucleation of new generations of droplets between existing drops. Thus, there is little information that can be derived from these earlier studies that applies to the case in which we are interested.

3. METHODS OF SIMULATION

3.1. Time Steps

Because of the underlying power law, it is convenient to work with a reduced time $\tau = (t/t_0)^a$, where t_0 is the initial time; the results of the simulation are then independent of the choice of the exponent a. The power-law nature of the basic growth process also leads naturally to the choice of a multiplicative time step. A guide for the magnitude of the time step can be derived from scaling arguments.[7] In the self-similar regime, the number of droplets is proportional to $\langle R \rangle^{-2}$ and, when coalescences are important, it can be anticipated that $\langle R \rangle$ grows as t^{3a}. Thus, we can define a time-step parameter

$$b = N(t_1)/N(t_2) = [\langle R(t_2) \rangle / \langle R(t_1) \rangle]^2 = (t_2/t_1)^{6a}$$

that sets an upper limit on the number of coalescences that can be expected within a time step.

The effect of the choice of time step was studied by varying b and by comparing simulations in which a constant value of b was utilized with those in which b was changed to maintain the fraction of coalescences per step essentially constant. Values of b from 1.02 to 2.2 were investigated. When an algorithm was used in which the search for coalescences always was carried out in the same order, there was a noticeable dependence on b during the late stages of the simulation. When the order of the search was randomized by "shuffling" the table of droplets between each step, however, values of b between 1.02 and 1.75 gave essentially identical results.

3.2. Initial configuration

A number of different methods have been employed to create the initial configuration. In the simplest case, which corresponds to an initial coverage of zero, 10,000 sites were placed randomly on a unit square. The sites were taken as the centers of equal-size disks whose radius was chosen empirically so that there would be some overlaps (i.e., coalescences) in the first time step.

Initial configurations at relatively high coverages could be generated by placing disks sequentially at random positions and rejecting coordinates that would result in overlaps. This procedure is quite time-consuming for coverages in excess of 45 % and an alternative scheme was also investigated in which droplets were initially placed on either a 100×100 square or hexagonal lattice. The system was then distorted by moving each disk a random distance and direction within a circle whose size was defined by the closest packing radius.

3.3. Polydispersity

In some of the simulations, polydispersity was introduced into the initial droplet distribution by choosing droplet radii with a Gaussian probability about the average radius. When the initial configuration was that of a distorted lattice, an upper bound to the radius was set by the requirement that disks fit within the circle defined by the closest packing radius; the lower bound was then chosen to make the distribution symmetric.

3.4. Procedure

The search for coalescences is carried out by calculating the distance between the centers of two disks and comparing it to the sum of the radii.

If the latter is larger, the two overlapping disks are replaced by one whose size and location are calculated as if the disks were median sections of hemispheres with conservation of volume and center of mass. To reduce computation time, the search for overlaps is confined to a square whose side length is four times the radius of the largest disk in the ensemble and which is centered on the disk being checked.

The computation time can also be markedly reduced by taking the center of the new disk to be center of the larger of the two overlapping disks. This procedure leads to coverages that are lower than those obtained when the new center corresponds to the center of mass. If one considers the conditions under which overlap with a third disk will result from coalescence of two disks, it becomes apparent (Fig. 1) that the probability of multiple coalescences (which reduce coverage) is lower if the center-of-mass location is used.

The fluctuations in the calculated properties of the ensemble of disks necessarily increase as coalescences cause the number of disks to decrease. One can reduce the fluctuations by increasing the initial number of disks, but it is more efficient to make several runs with the same initial conditions and to average them at each time step. In general each of our simulations is the average of 20 runs. The simulations were carried out on VAX 8600 and 780 computers.

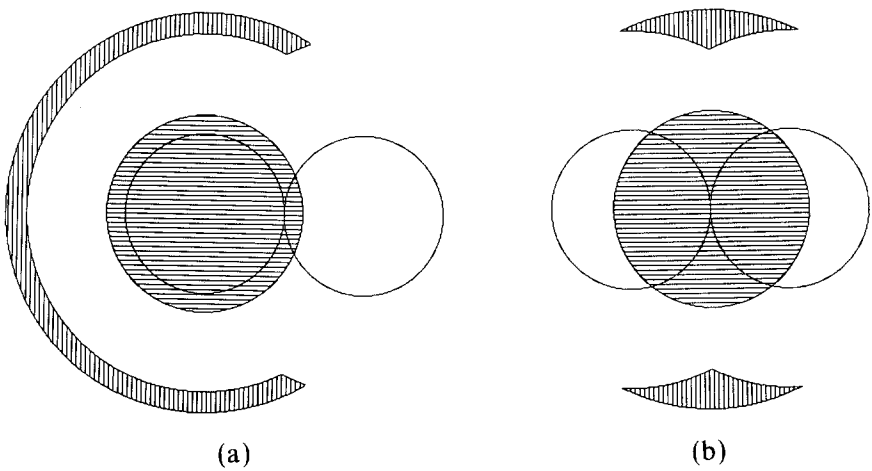

Fig. 1. Condition for coalescence with a third drop. Two droplets coalesce to form the droplet indicated by the horizontally hatched region. If the center of another droplet of the same size lies within the area indicated by the vertical hatch, an additional coalescence will then take place. (a) New droplet is centered on one of the coalescing pair. (b) New droplet appears at the center of gravity of the coalescing pair. It is evident that the chance of multiple coalescences is greater in (a).

4. RESULTS

It is convenient to define the reduced radius $\rho = \langle R \rangle / \langle R \rangle_0$, where $\langle R \rangle$ is the mass-averaged radius defined by $\sum r_i^3 / \sum r_i^2$ and $\langle R \rangle_0$ is its value at the initial time. Figure 2 shows the behavior of log ρ as a function of log τ for two systems that were initially monodisperse, one prepared at zero initial coverage and the other by random addition at an initial

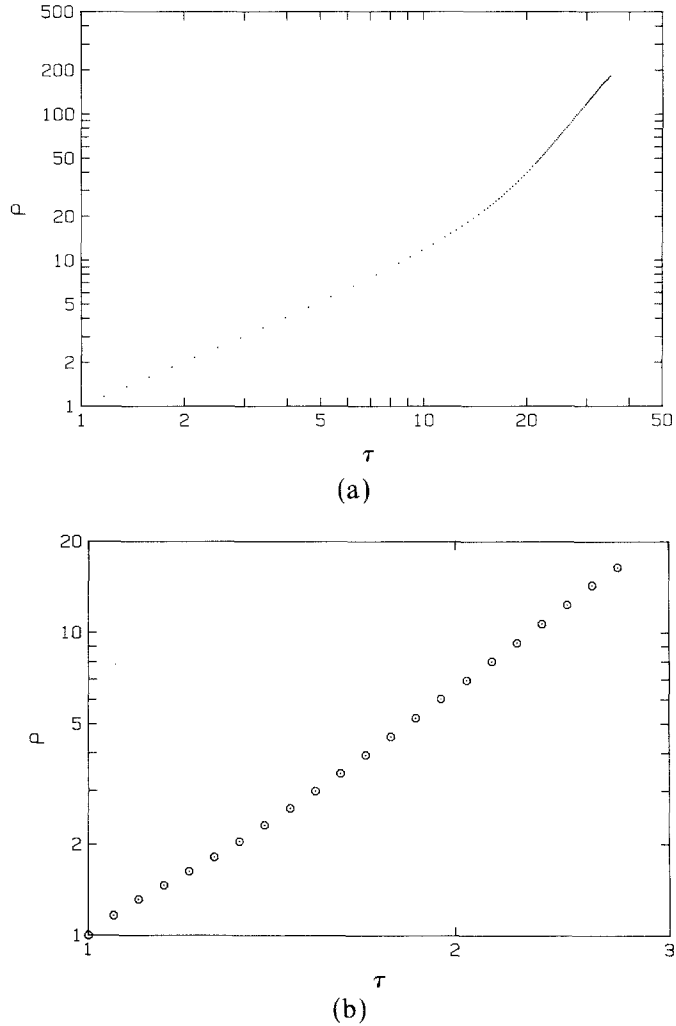

Fig. 2. Log–log plot of ρ against τ. (a) Random initial condition with zero initial coverage. (b) Random initial condition with coverage of 0.45. In both cases the systems were initially monodisperse.

coverage of 0.45. It is evident from Fig. 2a that there is an initial period during which the slope is unity, corresponding to single-particle power-law growth (i.e., $\langle R \rangle \propto t^a$) followed by a transition to a slope of 3, which corresponds to $\langle R \rangle \propto t^{3a}$. The t^a region of Fig. 2b is less clearly defined, but there is an obvious transition from one exponent to the other. This characteristic crossover from single-particle to coalescence-dominated growth is observed in all the simulations. It is unaffected by the choice of initial conditions, polydispersity, or procedure for drop replacement at coalescence.

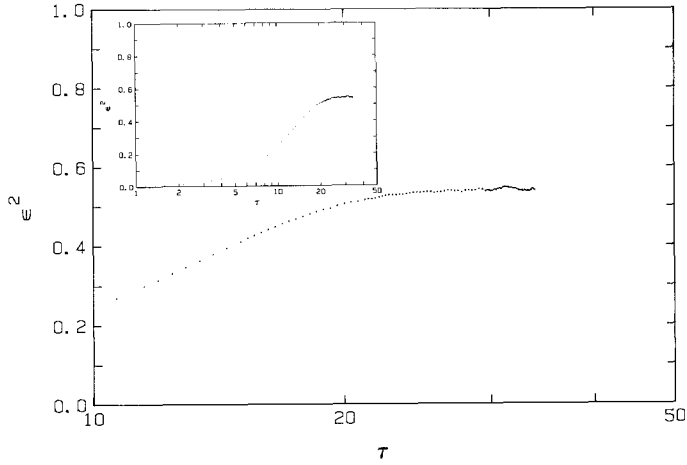

(a)

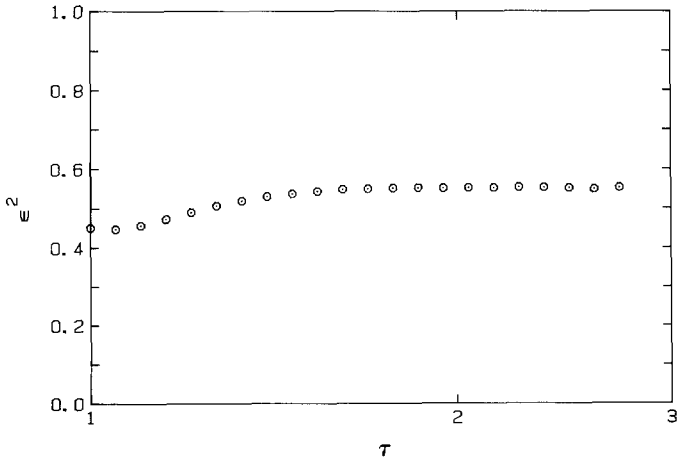

(b)

Fig. 3. Coverage ε^2 against log τ for the systems shown in Fig. 2. (a) Random initial condition with zero initial coverage. (b) Random initial condition with coverage of 0.45.

Plots of the coverage ε^2 against log τ for the systems shown in Fig. 2 are given in Fig. 3. After an initial rise, ε^2 levels off at a value of 0.57 and the time at which the transition to the plateau occurs corresponds to the change from single-droplet to coalescence-dominated growth. The mass-averaged polydispersity g,

$$g = (\langle r^2 \rangle - \langle r \rangle^2)^{1/2} / \langle r \rangle = \left[\sum r_i^2 \sum r_i^4 \Big/ \left(\sum r_i^3 \right)^2 - 1 \right]^{1/2}$$

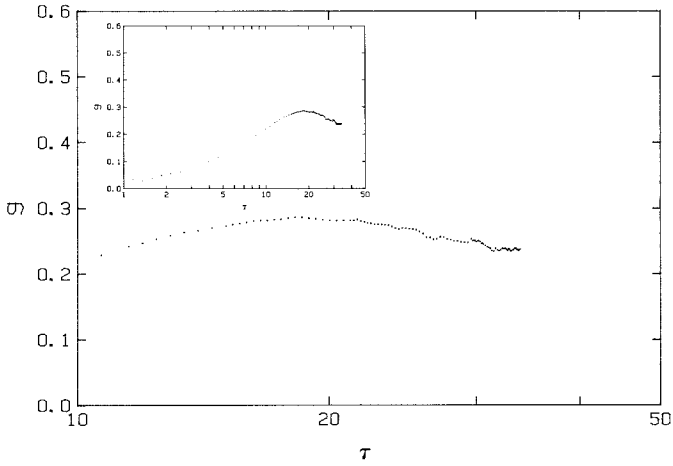

(a)

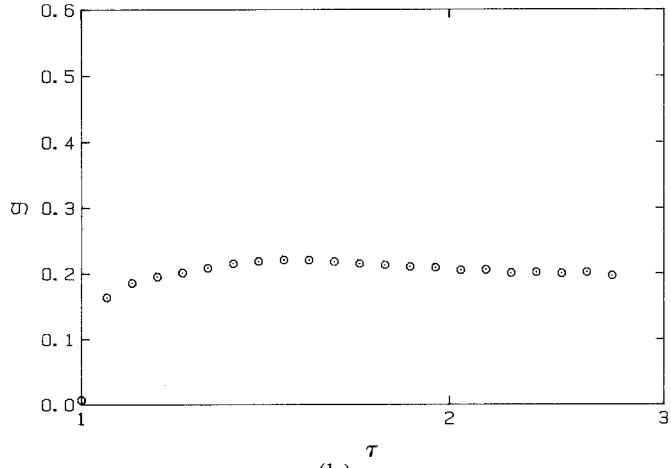

(b)

Fig. 4. Polydispersity g against log τ for the systems shown in Fig. 2. (a) Random initial condition with zero initial coverage. (b) Random initial condition with coverage of 0.45. Note that the maximum in (a) occurs at the time corresponding to the change in slope in Fig. 2a.

also shows this transition. As can be seen in Fig. 4, it rises through a small maximum to a plateau at a value of 0.16, where the transition in growth law takes place.

Although the qualitative behavior of ε^2 and g for other initial conditions and initial polydispersities is similar, there are quantitative differences. As the initial polydispersity is increased above 5 %, the maximum at early times becomes increasingly pronounced and the plateau region at later times becomes less well defined. The reason for this behavior becomes evident when one investigates size distributions. As shown in Fig. 5, which has been obtained from a simulation in which the initial value of the coverage was 45 % and the initial polydispersity was 30 %, the size distribution becomes bimodal because some of the disks do not undergo any coalescences. Disks that do not coalesce grow relatively slowly and account for an increasingly larger fraction of the total as coalescences reduce the number of the other disks.

A similar persistence of uncoalesced disks is found even for monodisperse systems if the initial coverage is low. In this case the effect of the uncoalesced disks is to decrease the length of the plateau region. Note that even a single uncoalesced disk eventually becomes important as the total number of disks decreases, but little physical significance can be

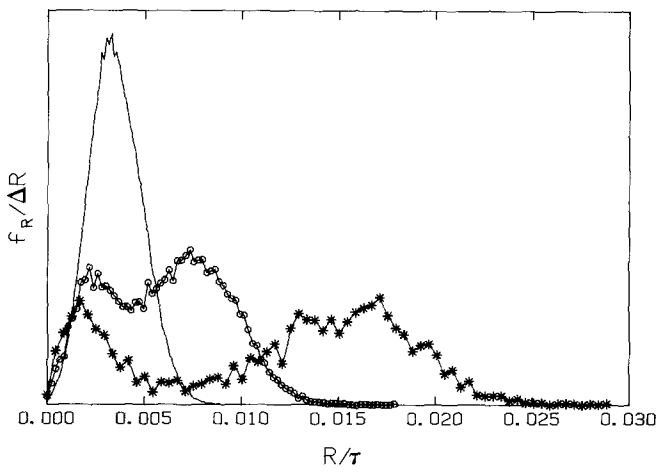

Fig. 5. Distribution of droplet sizes for a system with an initial polydispersity of 30 % and a coverage of 45 % at three times during the simulation. The areas under each of the curves have been normalized to unity. To facilitate the comparison, the ordinates have been normalized by the bin size ΔR, which is different for each curve, and the abscissa has been divided by τ to account for growth without coalescence. (—) $\tau = 1.14$; (○), $\tau = 1.80$; (★), $\tau = 2.55$.

attached to the average properties of systems that consist of just a few disks.

The conditions of constant coverage, constant polydispersity, and power-law growth of the average radius with an exponent $3a$ are characteristics of the self-similar regime observed in experiments[11] and discussed by Viovy *et al.*[7] A necessary condition for self-similarity is the scaling behavior of the structure factor, which is indicative of an underlying scaling of the pair distribution function. The average distance between disks is proportional to $N^{-1/2}$, which provides us with a characteristic length; we define a reduced distance $r^* = rN^{-1/2}$, where r is the radial distance from the center of a drop. The pair distribution function $g(r^*)$ is shown as a function of r^* in Fig. 6 for different times during the simulation that was the basis for Fig. 2a. At the start of the simulation, there is no correlation between the droplets and $g(r^*)$ is unity. As coalescences occur, the short center-to-center distances are preferentially eliminated and a short-range cutoff appears in the distribution function. At the same time, local order develops, as evidenced by the peak that arises in $g(r^*)$. As the system enters the regime in which the $3a$ growth law applies, the maximum in the peak increases and there is evidence of a second peak, indicating that the correlation is increasing. At longer times, the distribution function approaches the $g(r^*)$ for systems in which the coalescence mechanism is well developed.

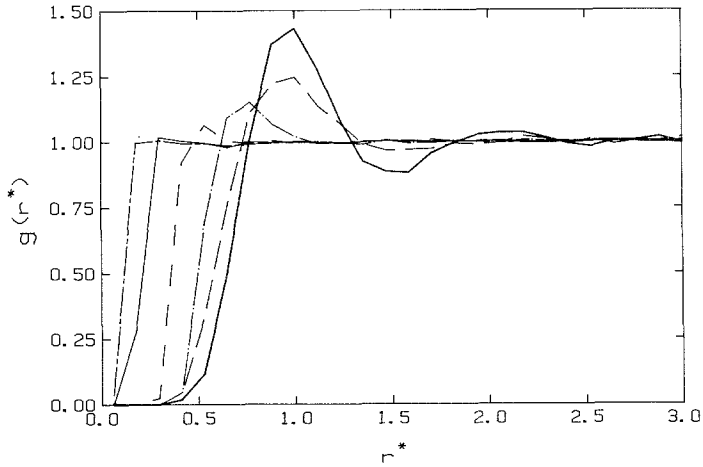

Fig. 6. Pair distribution function $g(r^*)$ against r^* at three times during the simulation shown in Fig. 2a. (- - -) $\tau = 1.8$, (—) $\tau = 3.4$, (– –) $\tau = 6.2$, (–·–) $\tau = 9.9$, (— —) $\tau = 17$. The heavy curve with the large maximum is for $\tau = 1.73$ in a simulation in which the initial coverage was 0.45.

The behavior in other simulations is comparable; once the $3a$ growth is well established, $g(r^*)$ does not change and the structure is therefore self-similar. The self-similarity breaks down in the late stages of the simulations when the number of droplets becomes small and the fraction of uncoalesced drops become significant. It is interesting to note that the peaks in $g(r^*)$ also appear when the coalescence is not accompanied by the moving of a droplet center. Thus, the local order is induced only by the process of coalescence and not by droplet movement.

5. COMPARISON WITH EXPERIMENTS

The simple model of growth and coalescence that we have employed in the simulations reproduces in detail the collective behavior observed in the experiments. Although the transition from the exponent a to $3a$ in the power-law growth of the *average* radius was not observed in the original experiments on clean, silanized glass slides,[5] it was inferred from experiments[11] in which there were isolated impurities on the surface of the slides and it has been confirmed in studies of the growth of droplets on the surface of a liquid.[12] The simulations make clear that correlation develops in an ensemble of coalescing droplets; it is not necessary that the initial state be highly compact. The appearance of a self-similar growth regime is also a natural result of the power-law growth and the coalescence process.

The numerical results of the simulations also agree remarkably well with those found in the experiments. It is notable that the plateau value of the coverage, 57 %, is close to the "jamming limit," the maximum coverage obtainable when monodisperse disks are placed randomly and sequentially on a two-dimensional surface with the requirement that there be no overlap. This process of random sequential adsorption has been much studied. The jamming limit in two dimensions has not been computed analytically, but Hinrichsen *et al.*[13] determined the value 0.547 ± 0.003 from computer simulations. We do not reach the same limit if the droplet formed by a coalescence is centered at the site of one of the coalescing pair. The essential difference between the two schemes for coalescence may be that the one in which the new droplet is located at the center of mass loses memory of the initial configuration while the other scheme does not. It should be noted that Rose and Glicksman[10] also suggested that the limiting coverage in droplet condensation is the jamming limit.

It is notable that the plateau value of the polydispersity also is closely similar to that found in the experiments. If the initial ensemble is monodisperse, the plateau value of the polydispersity represents the spread in sizes produced by the presence of several "generations" of disks at any

time once coalescence has begun. The agreement between the experimental values and those found in the simulation of monodisperse systems suggests that the initial distribution of droplets in the experiments has only a small spread in sizes, as it would if the surface was relatively uniform. The close agreement between the limiting coverage and the jamming limit for monodisperse disks also supports this view.

ACKNOWLEDGMENTS

This work was supported by National Science Foundation grant CHE 86 04038 and by NATO grant 86-0658. We thank Prof. Howard Reiss and Dr. Pierre Schaaf for making us aware of the jamming limit and its possible relation to our work.

REFERENCES

1. T. J. Baker, *Phil. Mag.* **44**:752 (1922).
2. R. Merigoux, *Rev. Opt.* **9**:281 (1937).
3. R. Merigoux, *C. R. Acad. Sci. Paris* **207**:47 (1938).
4. A. Brin and R. Merigoux, *C. R. Acad. Sci. Paris* **238**:1808 (1954).
5. D. Beysens and C. M. Knobler, *Phys. Rev. Lett.* **57**:1433 (1986).
6. E. E. Gose, A. N. Mucciardi, and E. Baer, *Int. J. Heat Mass Transfer* **10**:15 (1967).
7. J.-L. Viovy, D. Beysens, and C. M. Knobler, *Phys. Rev. A* **37**:4965 (1988).
8. I. Tanasawa and F. Tachibana, in *Proceedings Fourth International Heat Transfer Conference* (1970), Vol. 6, Paper Cs 1.3.
9. L. R. Glicksman and A. W. Hunt, Jr., *Int. J. Heat Mass Transfer* **15**:2251 (1972).
10. J. W. Rose and L. R. Glicksman, *Int. J. Heat Mass Transfer* **16**:411 (1973).
11. D. Beysens, D. Fritter, D. Roux, C. M. Knobler, and J.-L. Viovy, in *Proceedings International Symposium on Dynamics of Ordering Processes in Condensed Matter* (Kyoto, 1987).
12. C. M. Knobler and D. Beysens, *Europhys. Let.* **6**:707 (1988).
13. E. L. Hinrichsen, J. Feder, and T. Jossang, *J. Stat. Phys.* **44**:793 (1986), and references therein.